ELSEVIER

Functional incorporation of green fluorescent protein into hepatitis B virus envelope particles

Carsten Lambert[a], Nicole Thomé[a], Christoph J. Kluck[b], Reinhild Prange[a],*

[a]Department of Medical Microbiology and Hygiene, University of Mainz, D-55101 Mainz, Germany
[b]Biochemistry Center, University of Heidelberg, D-69120 Heidelberg, Germany

Abstract

The envelope of hepatitis B virus (HBV), containing the L, M, and S proteins, is essential for virus entry and maturation. For direct visualization of HBV, we determined whether envelope assembly could accommodate the green fluorescent protein (GFP). While the C-terminal addition of GFP to S trans-dominant negatively inhibited empty envelope particle secretion, the N-terminal GFP fusion to S (GFP.S) was co-integrated into the envelope, giving rise to fluorescent particles. Microscopy and topogenesis analyses demonstrated that the proper intracellular distribution and folding of GFP.S, required for particle export were rescued by interprotein interactions with wild-type S. Thereby, a dual location of GFP, inside and outside the envelope, was observed. GFP.S was also efficiently packaged into the viral envelope, and these GFP-tagged virions retained the capacity for attachment to HBV receptor-positive cells in vitro. Together, GFP-tagged virions should be suitable to monitor HBV uptake and egress in live hepatocytes.
© 2004 Elsevier Inc. All rights reserved.

Keywords: HBsAg particles; Hepatitis B virus; Green fluorescent protein; Viral envelope; Virus assembly and secretion

Introduction

Hepatitis B virus (HBV), a human hepadnavirus, is an enveloped DNA virus that infects hepatocytes and causes acute and chronic liver disease. Despite considerable understanding of the details of hepadnaviral genome replication, fundamental insights into the early and late steps of an HBV infection are still lacking. Infection initiates by virus attachment to the hepatocyte and is determined by the HBV envelope. Among the three related large L, middle M, and small S envelope proteins, L has been shown to play the key role in receptor recognition and cell attachment (Le Seyec et al., 1999; Neurath et al., 1986). The route of subsequent HBV uptake is a yet poorly identified process and may proceed by direct fusion of the viral envelope with the plasma membrane, receptor-mediated endocytosis, or alternate mechanisms (for review, see Cooper et al., 2003). In favor of a fusion mechanism at the cell surface is the previous demonstration of a pH-independent internalization of HBV in primary human hepatocytes (Hagelstein et al., 1997). By contrast, infectivity studies performed with the related duck HBV in duck liver cells have demonstrated that viral entry depends on endocytosis (Breiner et al., 1998).

In the late stages of an HBV infection, progeny virions are formed by budding of the pre-assembled cytosolic nucleocapsids, enclosing the partially double-stranded DNA genome 3.2 kb in length and the viral polymerase through intracellular membranes accommodating the viral envelope proteins (for review, see Nassal, 1996). During this process, an excess of envelope proteins is not incorporated into virion envelopes but self-assembles into secreted subviral lipoprotein particles referred to as hepatitis B surface antigen (HBsAg) particles or empty envelopes. These particles have been shown to mature by budding into intralumenal cisternae of post-endoplasmic reticulum (ER)–

pre-medial-Golgi compartments and to exit the cell by the constitutive secretory pathway (Huovila et al., 1992). In contrast, the intracellular budding site of viral particles has not been defined to date.

The three L, M, and S envelope proteins contribute differently to subviral and viral particle formation. Assembly and secretion of subviral particles are solely driven by the S protein and are initiated by co-translational integration of S molecules into the ER membrane (Simon et al., 1988). The current models for the transmembrane structure of S assume a lumenal disposition (i.e., external in the mature particles) of both the N- and C-termini and four membrane-spanning segments (Berting et al., 1995; Stirk et al., 1992). Following dimerization, about 100 transmembrane S monomers then self-assemble with host-derived lipids into spherical empty envelopes, 20 nm in diameter, which are secreted from the infected liver and transfected cell lines with high efficiency. This process is also sustained by the M protein that shares the sequence of S but differs in its N-terminal preS2 extension. By contrast, the L protein along with its N-terminal preS1 plus preS2 domains blocks subviral particle production but is the key player in virion formation (Bruss and Ganem, 1991; Chisari et al., 1986). The pivotal role of the L protein in the viral life cycle is related to its dual transmembrane topology (Bruss et al., 1994; Ostapchuk et al., 1994; Prange and Streeck, 1995), as its internal (cytosolic) preS domain is needed for envelopment of cytosolic nucleocapsids (Bruss et al., 1996), while the same external (lumenal) preS domain mediates receptor binding during host cell attachment (Le Seyec et al., 1999).

In the present study, we addressed whether the HBV envelope could be tagged with the green fluorescent protein (GFP) without impairing its functionality. We reasoned that such GFP-tagged particles should be a promising tool to study the early and late stages of the HBV life cycle in live cells.

Results

N-terminal but not C-terminal addition of GFP to S allows co-integration into empty envelopes

For tagging of the HBV envelope with GFP, the S protein was chosen as the target because this protein is an essential and abundant constituent of the virion envelope. Two chimeras were constructed by fusing either a fluorescence-enhanced GFP in frame to the N-terminus of S (GFP.S) or the yellow-shifted YFP variant to the C-terminus of S (S.YFP) (Fig. 1A). The fusion constructs were transiently expressed in COS-7 cells and analyzed by GFP-specific Western blotting. The unfused S protein with a C-terminal HA-tag (SHA) was included as reference. As shown in Fig. 1B, lysates of cells contained SHA in its characteristic doublet of a non-glycosylated (p24) and single-glycosylated (gp27) form as a consequence of partial modification at
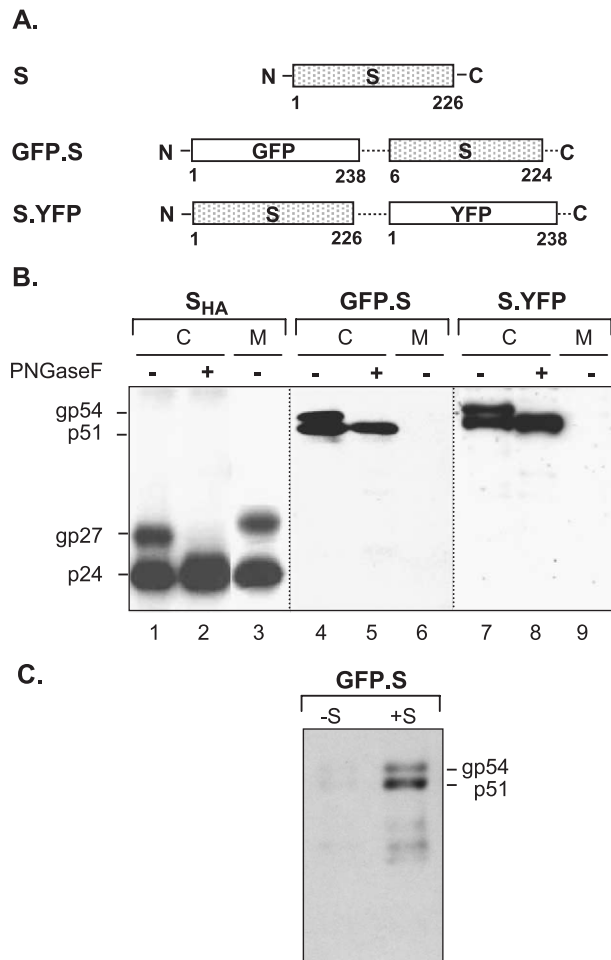

Fig. 1. The N-terminal GFP.S fusion is co-secreted with wild-type S. (A) Schematic representation of the HBV S protein and the GFP.S and S.YFP fusion constructs. Numbers below the domains refer to the corresponding amino acid positions of S (hatched bar) and GFP/YFP (white bars). For GFP.S, the two domains are linked by the amino acid sequence SGLRSRAQASN and terminated by the extra sequence WDPPDLDN, while S and YFP are interspersed by the sequence DPPVAT. (B) Synthesis, glycosylation, and secretion of SHA and the fusion constructs. Lysates (C) from transfected COS-7 cells were divided into two portions and either left mock treated or digested with PNGase F, as indicated. Cellular supernatants (M) were analyzed without enzymatic de-glycosylation. Proteins were processed by SDS-PAGE and HA-specific (lanes 1–3) or GFP-specific (lanes 4–9) immunoblotting. Nonglycosylated (p) and glycosylated (gp) forms are indicated on the left with the numbers referring to the molecular masses of the polypeptides. (C) Secretion of GFP.S is rescued by co-expressed wild-type S molecules. Supernatants of cells synthesizing GFP.S in the absence (−) or presence (+) of S were assayed by GFP-specific Western blotting.

Asn-146. N-linked glycosylation was confirmed by treatment with peptide/N-glycosidase F (PNGase F), which converted the gp27 form of S to its faster migrating p24 form. The GFP.S and S.YFP fusion proteins were stably expressed as 51-kDa polypeptides in accordance with the molecular masses calculated for their non-glycosylated forms (p51) (Fig. 1B). As evidenced by enzymatic de-glycosylation, both fusion proteins appeared in glycosylated forms (gp54) in addition, indicating that they were

competent for co-translational integration of the S region into the ER lumen. However, unlike wild-type SHA, each chimera failed to be secreted from transfected cells into the supernatants (Fig. 1B).

Although these results implicated some misfolding of GFP.S and S.YFP, we nonetheless assessed whether their block to secretion could be abrogated by co-expression of wild-type S. COS-7 cells were co-transfected with each fusion construct, and the wild-type vector at a ratio of 1:1 and cellular supernatants were assayed by GFP-specific immunoblotting. The S.YFP fusion turned out to act in a *trans*-dominant-negative manner and even inhibited export of co-expressed wt S chains (data not shown). By contrast, GFP.S was secreted in the presence of S (Fig. 1C), and thus was chosen for further analysis. For quantitative evaluation of the secretion efficacy of GFP.S, lysates and supernatants of GPF.S + S co-transfected cells were analyzed with a GFP-specific ELISA. This determination revealed that $68 \pm 5.2\%$ of the intracellular GFP.S was released into the supernatant when co-expressed with wt S.

GFP.S localizes to the ER if co-expressed with wild-type S

In order to get insights how S rescued the secretion of GFP.S, we comparatively examined the intracellular distribution of GFP.S in the presence and absence of SHA. When expressed alone, GFP.S surprisingly yielded an intense micropunctate fluorescence (Fig. 2a). These "dots" partially overlapped with ER structures, as shown by co-staining of

the cells with antibodies to the ER-resident protein disulfide isomerase (PDI) (Figs. 2b and c). Although the nature of these structures remained to be determined, they might present aggregates of malfolded GFP.S destined for degradation. Importantly, however, on co-expression of GFP.S with SHA, the chimera now exhibited a widely dispersed membranous staining pattern together with a significant co-localization with the ER marker PDI (Figs. 2d–f). Under the same conditions, a nearly 100% co-localization of GFP.S with SHA was observed when cells were stained with HA-specific antibodies (Figs. 2g–i). From these data we concluded that the correct distribution of GFP.S, required for export, was warranted by interaction with co-expressed S chains.

Incorporation of GFP.S into envelopes produces fluorescent subviral particles

To determine whether the co-secreted GFP.S and SHA proteins resembled authentic subviral HBV envelope particles, the culture supernatant of transfected cells was fractionated by isopycnic CsCl gradient centrifugation and fractions were analyzed by an S-specific ELISA. As shown in Fig. 3A, the co-secreted proteins banded at a buoyant density of about 1.22 g/ml, typical for wild-type S lipoprotein particles (Heermann and Gerlich, 1991). Peak fractions were then subjected to specific Western blot analysis that confirmed the presence of both the GFP.S fusion and the SHA protein (Fig. 3A). In addition, when
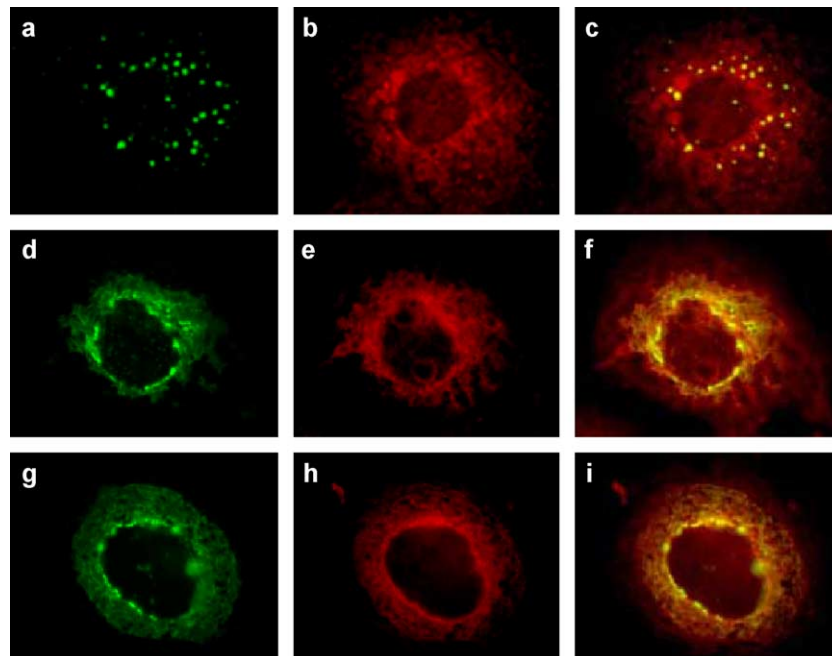

Fig. 2. GFP.S co-localizes with wild-type S at the ER. Shown is the intracellular distribution of GFP.S expressed either alone (squares a–c) or together with SHA (squares d–i) in COS-7 cells. Cells were fixed, permeabilized, and examined by fluorescence microscopy. (a, d, and g) GFP fluorescence (green); (b and e) immunostaining with a mouse antibody to PDI followed by AlexaFluor 494-conjugated goat anti-mouse IgG (red); (h) immunostaining with a mouse anti-HA antibody followed by AlexaFluor 494-conjugated goat anti-mouse IgG (red) to visualize SHA. Squares c, f, and i are the corresponding merged images so that overlapping red and green signals appear yellow.
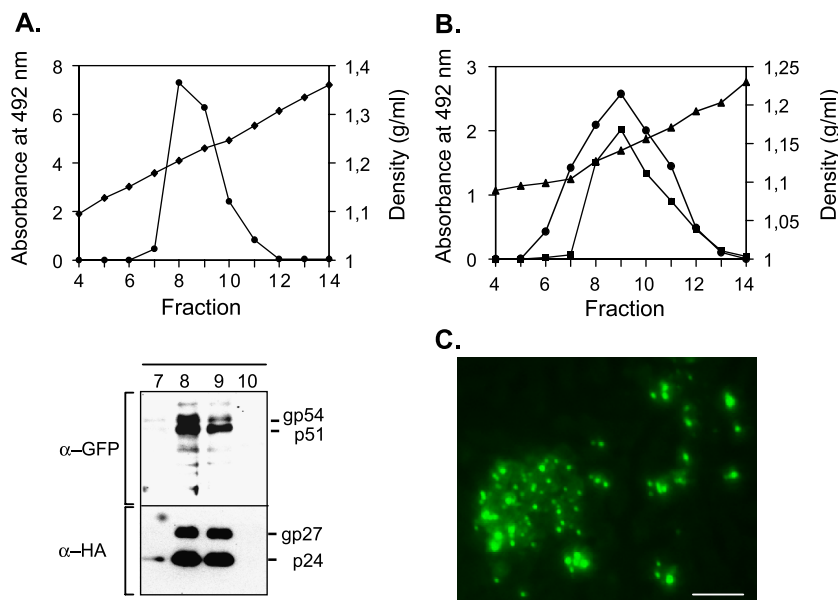
Fig. 3. Co-assembly of GFP.S and wild-type S into fluorescent lipoprotein particles. (A) Concentrated cell culture media of GFP.S + SHA co-transfected cells were analyzed by CsCl density centrifugation. Gradients were fractionated from the top and each fraction was assayed for HBsAg by ELISA (-●-). The peak fractions 7–10 were subjected to SDS-PAGE; the upper part of the blot was reacted with α-GFP, the lower part with α-HA antibodies. (B) For velocity sedimentation analysis, concentrated supernatants of SHA (-■-) or GFP.S + SHA (-●-)-transfected cells were assayed by sucrose gradient centrifugation. After fractionation from the bottom, fractions were probed for HBsAg particles by ELISA. (C) Autofluorescence of GFP.S + SHA particles. Supernatants of co-transfected cells were concentrated 50-fold by centrifugation through a 20% sucrose cushion. Pelleted particles were spotted on glass bottom dishes, visualized by fluorescence microscopy, and photographed at 1600× magnification. Scale bar = 5 μm.

GFP.S + SHA and wild-type SHA particles were analyzed by sucrose gradient velocity centrifugation, their sedimentation profiles were nearly coincident with a buoyant density of about 1.130 g/ml in sucrose (Fig. 3B). Together, these data demonstrated that GFP.S was successfully incorporated into subviral particles that closely resembled S spheres with respect to density and size.

Because the fluorescence of GFP depends on its native three-dimensional structure that might be altered within the chimeric context, we next examined whether purified GFP.S + SHA particles were fluorescent. As imaged by fluorescence microscopy, a strong vesicular GFP staining was observed, indicating a native display of GFP within the particle (Fig. 3C). The intensity of fluorescence and hence the apparent size of the particles appeared slightly variable and brighter than expected, perhaps because of some particle aggregation or variation in the amount of GFP.S incorporation.

GFP.S forms a split topology if co-expressed with wild-type S

The production of fluorescent subviral particles indicated that the individual constituents of the GFP.S chimeric protein were properly folded, at least when co-expressed with wild-type S chains. Nonetheless, for further studies outlined below, it was important to know its precise topology, that is, the orientation of the GFP domain relative to the membrane. According to current models for the transmembrane structure of S, its N-terminus and hence the

GFP fusion site are located to the lumenal side of intracellular membranes that is topologically equivalent to the virion surface (Fig. 4A) (Berting et al., 1995; Stirk et al., 1992). To analyze the topological features of GFP.S, expressed in the absence or presence of S molecules, we used proteinase K protection experiments of microsomes prepared from transfected COS-7 cells. Both GFP.S and S proteins were synthesized in HA-tagged form to enable their simultaneous detection by immunoblotting. Consistent with previous works (Wunderlich and Bruss, 1996), proteinase K did not cleave the p24/gp27 forms of SHA unless the protecting microsomal membrane was disrupted by detergent (Fig. 4B, lanes 4–6). By contrast, GFP.SHA synthesized in the absence of SHA chains was accessible to cleavage with the protease in intact microsomes (Fig. 4B, lanes 1–3). Thereby, two HA-reactive fragments were generated that closely resembled the full-length p24 and gp27 forms of SHA. Therefore, cleavage of GFP.SHA must have occurred at least at a very distal site within the N-terminal fused GFP domain. In support of a fully cytoplasmic location of the GFP domain, we were unable to detect GFP-reactive proteolysis products by Western blotting (data not shown). When expressed together with SHA, the topology of GFP.SHA surprisingly changed in such that a fraction of polypeptides was now protected from cleavage with proteinase K by the microsomal membrane (Fig. 4B, lanes 4–6). These results indicated that the presence of extra SHA chains caused a partial topological change of the N-terminal GFP domain from cytosolic to lumenal, likely as a consequence of GFP.SHA/SHA
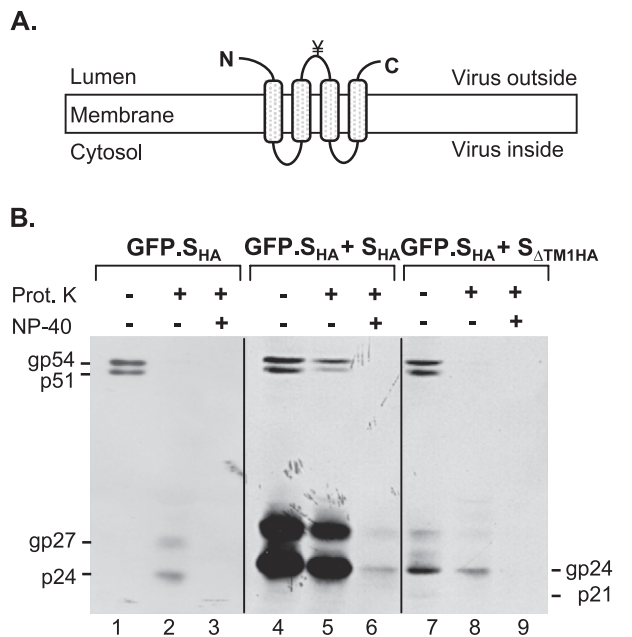
A.

B.

Fig. 4. GFP.S forms a mixed topology when co-expressed with wild-type S. (A) Model of the transmembrane topology of S at the ER membrane and the virion envelope. The predicted four membrane spanning segments of S project its N- and C-terminus into the ER lumen that is topologically equivalent to the virus outside. The N-glycosylation site at Asn-146 is indicated by ¥. (B.) Proteinase K protection assay of GFP.S. COS-7 cells were transfected with HA-tagged GFP.S either alone (lanes 1–3) or together with HA-tagged S (lanes 4–6) or the secretion-defective SΔTM1 mutant (lanes 7–9). Two days after transfection, microsomes were prepared and either left untreated or digested with Proteinase K (Prot. K) in the absence (−) or presence (+) of NP-40, as denoted above each lane. Samples were analyzed by HA-specific immunoblotting. The GFP.S- and S-specific p and gp forms are indicated on the left; the corresponding forms of SΔTM1HA are denoted on the right.

interprotein subunit interaction. Given the strict correlation between partial N-tail translocation and secretion competence and vice versa, we finally investigated the topological properties of GFP.SHA complemented in trans with a secretion-defective S mutant protein. To this aim, we took advantage of SΔTM1HA that lacks the first transmembrane domain and is blocked in the assembly and secretion of subviral particles (Prange et al., 1992). Consistent with our previous results (Prange et al., 1992), the deletion mutant predominantly appeared in a glycosylated 24-kDa form (gp24; Fig. 4B, lane 7). Importantly, SΔTM1HA failed to impart a partial lumenal orientation of GFP.SHA (Fig. 4B, lanes 7–9). Together, these data indicated that the topological change of GFP.SHA in the presence of extra S molecules was likely established during the formation and extracellular release of the GFP.SHA/SHA mosaic particles.

If this notion was correct, we would expect the GFP tag located outside and inside of the secreted particle. For a formal proof of a surface display of the GFP domain, we tried to immunoprecipitate the particles under non-denaturing conditions using two monoclonal α-GFP antibodies directed against different epitopes. However, neither antibody brought down the particles in the absence of detergent

(data not shown; and see below). Although these results might argue against an exterior location of GFP, it seemed equally possible that the epitopes were not accessible in the bulky beta barrel of GFP on the intact particle.

Incorporation of GFP.S into envelopes allows viral particle formation

Next we examined whether GFP.S would also be incorporated into the viral envelope. For virus production, human hepatoma HuH-7 cells were transiently transfected with a cloned over-length copy of the HBV genome. On co-transfection with the GFP.S expression plasmid at a 1:1 ratio, virus secretion into the cellular supernatant was reduced about 3-fold (data not shown), whereas no inhibitory effect of GFP.S on the virus secretion profile was observed if a 4-fold excess of the HBV encoding vector was used for co-transfection. Because transfected HuH-7 cells released viral and subviral particles into the culture medium, virions were separated from empty envelope particles by isopycnic CsCl gradient centrifugation. A resolution of these particle types was verified by assaying of fractions for the presence of HBV DNA by the endogenous polymerase reaction. As shown in Fig. 5 (A and B), DNA-containing virions banded at a density near 1.24 g/ml around fractions 18–22, with the strongest signal in fraction 20, while empty envelopes were found at their typical density of 1.22 g/ml. Importantly, when probed with a GFP-specific ELISA, the virus-containing fractions were clearly reactive, thus giving first hints to an incorporation of the GFP-tagged S protein during virus assembly. As a final proof, supernatants of HBV + GFP.S co-transfected HuH-7 cells were immunoprecipitated with a GFP-specific antibody prior to detection of the viral genome by dot-blot analysis. For reasons mentioned above, such a precipitation, however, required the presence of detergent (0.5% NP-40) that decreased the limits of detection, likely because some nucleocapsids might leak from the disordered envelope network. Nonetheless, despite these restraints, we could specifically detect the viral DNA in α-GFP-precipitated supernatants (Fig. 5C).

Incorporation of GFP.S into envelopes allows virus attachment to liver cells

To investigate whether these fluorescent HBV virions supported attachment to hepatocytes, cell binding assays were performed. Although most permanent cell lines are not permissive to HBV infection, the human hepatoblastoma HepG2 cell line is able to bind the virion (Lu et al., 1996). For binding, we applied the same assay conditions as validated previously for in vitro infection of primary human hepatocytes (Gripon et al., 1993). Accordingly, recombinant HBV + S.GFP particles secreted from co-transfected HuH-7 cells (see above) were precipitated with polyethylene glycol (PEG) and reacted with HepG2 cells grown on glass bottom
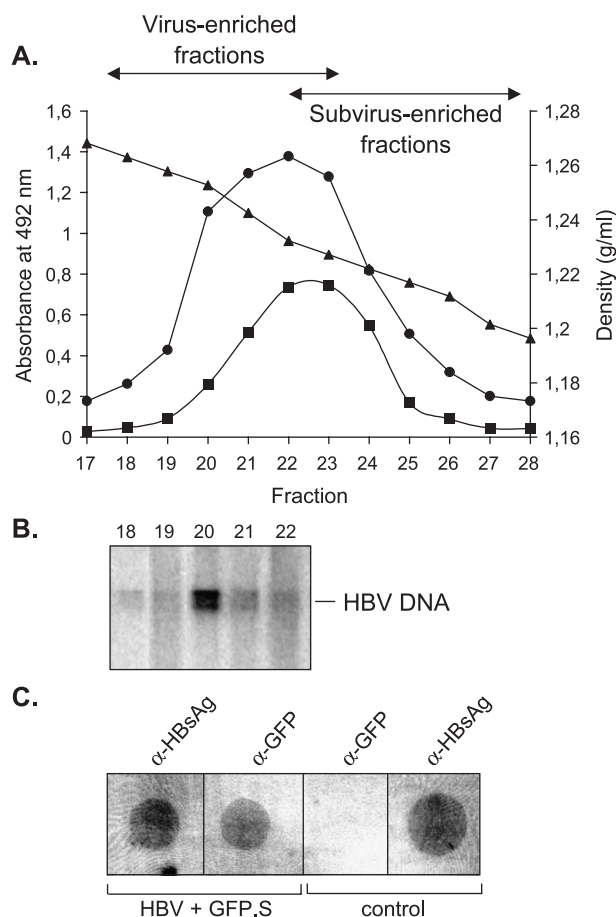
A.

B.

C.

Fig. 5. GFP.S is incorporated into the virus envelope. (A) Viral and subviral particles secreted from HBV + GFP.S co-transfected HuH-7 cells were separated by isopycnic CsCl gradient centrifugation according to their buoyant densities (-▲-). Fractions were analyzed by enzyme immuno-assays for HBsAg (-■-) and GFP (-●-), as indicated. (B) Fractions 18–22 containing virion particles were further subjected to an envelope-specific immunoprecipitation and radioactive labeling of the viral genome by the endogenous viral polymerase. The migration of the HBV DNA genome as visualized by agarose electrophoresis and PhosphorImaging is indicated. (C) Pooled extracellular viral particle fractions from HBV + GFP.S co-transfected cells were immunoprecipitated with either an envelope-specific (α-HBsAg) or a GFP-specific (α-GFP) antibody prior to extraction of the viral genome and DNA dot blot analysis. For control of nonspecific immunoprecipitation, native HBV particles (control) were reacted with the α-GFP MAb (third panel from the left). In addition, the control material was probed with α-HBsAg, as shown in the right panel.

dishes. After incubating cell cultures overnight, followed by several washes, a strong GFP fluorescence almost evenly distributed on the plasma membrane of the hepatocytes was observed (Figs. 6a and b). To test the specificity of adsorption, we analyzed the binding properties of GFP.S + S subviral particles that lacked the L envelope protein and thus the receptor binding site. As expected, these particles failed to attach to HepG2 cells thereby yielding only some diffuse background staining (Figs. 6c and d). However, because infected liver cells and HBV-producing cell lines are known to also produce subviral particles containing the L protein (Nassal, 1996), we could not totally exclude the

possibility that the GFP fluorescence, shown in Figs. 6a and b, might be also generated by binding of this particle type.

Discussion

In recent years, the adaptation of the *Aequorea Victoria* GFP for visualization of protein expression and protein localization in living organisms has provided a powerful new tool. Here we applied this approach to hepatitis B virus and obtained fluorescent subviral and viral particles by incorporation of the viral S envelope protein, tagged with GFP, in trans, thereby preserving all the functions necessary for the viral life cycle.

Because HBV empty envelope particles, built from the S protein, provide a safe antigen delivery system, their use as a carrier for the presentation of various antigens is a long established practice. To date, chimeric particles have been produced in mammalian cells with inserts in the range of 10–80 amino acids (Delpeyroux et al., 1986; Michel et al., 1988; Prange et al., 1995). For example, the N-terminal ectodomain of the S protein has been shown to tolerate 84 foreign residues while its C-terminus accommodated 42 residues without effects on particle assembly and secretion (Michel et al., 1988; Prange et al., 1995). In agreement and extension, the current study demonstrated that the N-terminus of S is more permissive for insertions than the C-terminus and is even amenable for addition of the complete GFP protein. Hence, proteins of at least up to 238 amino acids can be displayed on HBV envelope
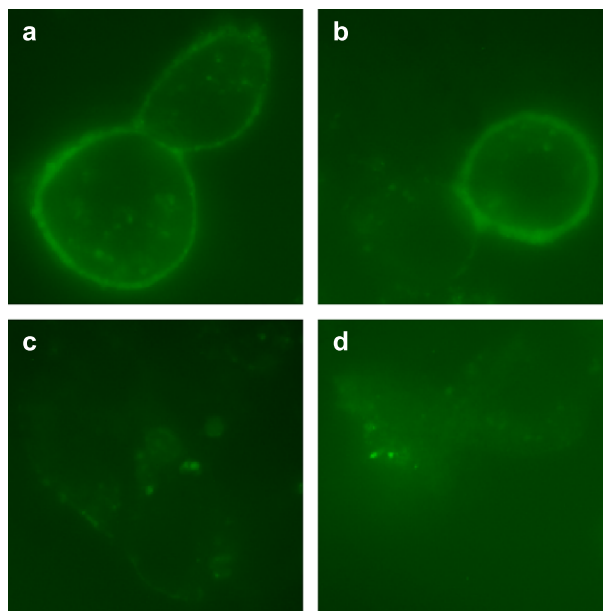

Fig. 6. GFP-tagged HBV binds to HepG2 cells. In squares a and b are shown the adsorption of GFP-tagged HBV particles (HBV + GFP.S) to live HepG2 cells, grown on glass bottom dishes, as detected by GFP autofluorescence (magnification, ×1600). Under the same assay conditions, GFP-tagged subviral particles (S + GFP.S) did not bind to cells (squares c and d).

particles, raising intriguing perspectives for their future use as a carrier system.

Particle formation of the GFP.S chimeric protein, however, depended on the presence of the wild-type S protein, indicating that the fusion construct itself failed to fold into a functional conformation required for assembly. Nonetheless, as judged by the autofluorescence of GFP.S in cells, at least the GFP-tag must have folded properly. Thereby, GFP.S surprisingly appeared in sequestered speckles that overlapped with the ER compartment. The formation of similar structures, termed concentric membranous ER bodies, has been recently observed upon expression of a misfolded mutant of the cystic fibrosis transmembrane conductance regulator that accumulates in these bodies prior to ER-associated degradation (Okiyoneda et al., 2004). Accordingly, the S moiety of GFP.S might not attain its native transmembrane structure thereby tending to aggregate into discrete speckles. On co-expression with wild-type S, the intracellular distribution of GFP.S completely changed in such that it now yielded a typical membranous ER staining pattern and a high degree of co-localization with S. This result indicates that the proper folding and localization of GFP.S were warranted by interprotein interactions with wild-type S chains. As a consequence thereof, highly fluorescent mosaic particles were formed and secreted, which closely resembled authentic spherical S lipoprotein particles according to density and size.

Furthermore, the GFP.S fusion protein could be also natively incorporated into the virion envelope. GFP, by virtue of its properties, has been successfully used to tag various viruses like, for example, herpes simplex virus type I, vesicular stomatitis virus, vaccinia virus, HIV, and mouse hepatitis coronavirus (Bosch et al., 2004; Dalton and Rose, 2001; Desai and Person, 1998; Stauber et al., 1999; Ward and Moss, 2001). However, unlike these viruses, HBV is a very small particle with a diameter of 42 nm and a dense packed structure. Even so, it can apparently accommodate multiple copies of GFP, indicating that there is substantial space available between the viral envelope and the nucleocapsid as well as sufficient flexibility allowing the incorporation of proteins in trans. Although we were unable to unequivocally define the location of the GFP-tag within the secreted HBV envelope, our topological analysis of GFP.S suggested an interior (i.e., cytosolic side of microsomes) and exterior (i.e., lumenal side of microsomes) display of GFP. The formation of such a mixed topology is rare among membrane proteins but is a prominent feature of the large L envelope protein of HBV (Bruss et al., 1994; Ostapchuk et al., 1994; Prange and Streeck, 1995). In that case, it is established post-translationally at the ER membrane and is uncoupled from envelope assembly (Lambert and Prange, 2001). By contrast, the two differently orientated isoforms of GFP.S were only generated upon co-expression with secretion-competent wild-type S molecules, thus hinting to a link between envelope subunit interactions and topogenesis of GFP.S. While the underlying mechanism remains to be determined, it is tempting to speculate that the dual location of the GFP domain might be beneficial for the functionality of GFP-tagged HBV. By splitting the tag to both sides of the virion envelope, the local density of GFP might be lowered thereby limiting the risk of sterical hindrance of the envelope/nucleocapsid interactions at the interior and the envelope/receptor binding at the exterior.

By using HepG2 cells, an established hepatocyte-derived cell line that is permissive for HBV attachment but non-permissive to a productive infection (Lu et al., 1996), a specific binding of GFP-tagged viral particles was observed. Hence, these particles must imitate the natural virus and viral attachment appeared to proceed through the authentic pathway. However, whether these particles even retained their infectivity remains to be addressed. In vitro HBV infection studies had been restricted to primary human hepatocytes that are not readily available. More recently, however, successful experimental infections of tree shrews were carried out that might present a new animal model (Köck et al., 2001). In addition, a human hepatoma cell line has been established that supports HBV infection (Gripon et al., 2002). Therefore, the GFP-tagged HBV envelope might be useful for the investigation of the early events of virus penetration such as monitoring entry and uncoating in living infected cells and tracing the fate of the envelope structure. With GFP as a marker, it should also be possible to approach sites of viral assembly and to follow the intracellular trafficking and egress of (sub)viral particles during the late stages of an HBV infection.

Materials and methods

Plasmid constructions

The mammalian expression vectors carrying the HBV S gene with or without a C-terminally tagged influenza virus hemagglutinin (HA) epitope under the control of the human metallothionein IIA promoter had been described (pNI2.-SHA and pNI2.S, respectively) (Hartmann-Stühler and Prange, 2001). For construction of the GFP.S chimera, plasmid pEGFP-C1 (BD Biosciences Clontech) was cut within the multiple cloning site by using EcoRI and SmaI. To introduce an EcoRI restriction site downstream of the start codon of the HBV S gene, site-directed mutagenesis with a recombinant M13mp19 bacteriophage carrying a 2.3-kb BglII–BglII fragment (nucleotide [nts] 2839 to 1986, as referred of the HBV genome, subtype ayw) with the anti-sense oligonucleotide 5′-GAATCCTGAATTCATGTTCTC-3′ (the EcoRI site is italic) was performed. The newly created EcoRI site, cutting between codon positions 4 and 5 (nts 170) of the S gene, together with the cognate filled-in AccI site (nts 827) was then used to generate an S encoding fragment for in-frame insertion into pEGFP-C1, giving rise to plasmid pEGFP.S. In parallel, the HA-tagged version of the S gene was similarly cloned, giving rise to GFP.SHA. A

reciprocal chimera, containing the yellow-shifted YFP co-linearly fused to the C-terminus of S (S.YFP), was created using plasmid pEYFP-N1 (BD Biosciences Clontech), which was opened with *Xho*I and *Bam*HI. The HA-tagged S gene was derived from pNI2.SHA by cleavage with *Xho*I (nts 127) and *Psi*I (cutting between the HA-tag and the translational stop codon) and inserted into pEYFP-N1 after filling-in of its *Bam*HI site. Plasmid pNI2.SΔTM1HA carries an in-frame deletion of TM1 that was achieved by removal of a *Sty*I (nts 180)–*Xba*I (nts 249) fragment from pNI2.S.

Cell culture, transfection, and immunoblotting

To produce viral envelope proteins, transient transfection of COS-7 cells by electroporation was used. Unless otherwise indicated, 5×10^6 cells were transfected with 12 μg of plasmid DNA, while in the case of co-transfections, 12 μg of each DNA was used. Three days post-transfection, cellular supernatants were harvested and clarified by low-speed centrifugation. Cells were washed twice in Tris-buffered saline (TBS, 50 mM Tris–Cl [pH 7.5], 150 mM NaCl) and lysed with 1 ml of TBS–0.5% Nonidet P-40 (NP-40), supplemented with a protease inhibitor cocktail (Roche), for 30 min on ice. After centrifugation for 5 min at $13\,000 \times g$ and 4 °C, proteins of lysates and cell supernatants were precipitated with 10% trichloroacetic acid (TCA), washed twice with 5% TCA, and once with acetone. TCA precipitates were resolved by SDS-PAGE and Western blotted to nitrocellulose membranes. Enzymatic N-deglycosylation of proteins with PNGase F (New England Biolabs) was done according to the instructions of the supplier. Immunoblots were incubated with a mouse monoclonal antibody (MAb) against the HA epitope (BabCO), diluted 1:2000 in blotting buffer (PBS with 5% skim milk) or a mouse MAb specific for GFP (JL-8; BD Biosciences Clontech) applied in 1:4000 dilution. Peroxidase-labeled secondary antibodies (Dianova) were diluted as instructed by the manufacturer, and the blots were developed with enhanced chemiluminescence detection reagents (Amersham Biosciences).

Immunoassays

In parallel, cell lysates and supernatants were analyzed by ELISAs. HBsAg was measured using the Auszyme II diagnostic kit (Abbott Laboratories). For simultaneous detection of GFP and HBsAg, a sandwich ELISA with GFP-specific antibodies in the solid phase and S-specific antibodies in the detection phase was employed. Briefly, the α-GFP-MAb JL-8 was coated to microtiter plates (1:500 dilution in TBS) for 3 h at room temperature. Nonspecific binding sites were blocked with TBS–1% bovine serum albumin for 18 h at 4 °C, followed by three washes with TBS–0.1% Tween 20. Samples were reacted for 2 h at 37 °C in the presence of 0.5% NP-40, washed out, and incubated

with peroxidase-labeled HBsAg-specific MAbs (Auszyme II) for 1 h at 37 °C.

GFP fluorescence and immunofluorescence assays

Transfected COS-7 cells on glass cover-slips were fixed and permeabilized with ice-cold methanol containing 2 mM EGTA for 15 min at −20 °C. For staining of internal antigens, cells were incubated with the HA-specific MAb (1:200 dilution in PBS) or a mouse MAb specific for protein disulfide isomerase (SPA-891, StressGen Biotechnologies) (1:2000 dilution in PBS) prior to incubation with an AlexaFluor 594-conjugated goat anti-mouse immunoglobulin G (2 μg/ml in PBS; Molecular Probes). Spontaneous GFP fluorescence and immunostaining were visualized with a fluorescence microscope (Axiovert 200M, Zeiss), and images obtained with a Zeiss AxioCam digital camera were processed using the Zeiss Axiovision software. To assess for fluorescent particles, cellular supernatants were concentrated 50-fold by ultracentrifugation (see below). A 10-μl aliquot was spotted on glass bottom dishes (BD Biosciences), briefly air dried, and imaged with a ×100 objective.

Proteinase K protection assay

Three days after transfection of COS-7 cells, microsomes were prepared essentially as described (Prange and Streeck, 1995). Briefly, cells were disrupted by dounce homogenization, and microsomes were recovered by ultracentrifugation prior to proteolysis with proteinase K (100 μg/ml) in the presence or absence of 0.5% NP-40. After incubation on ice for 60 min, proteinase K was inactivated by the addition of 10 μl/ml phenylmethylsulfonyl fluoride. Each sample was then adjusted to 0.5% NP-40 and solubilized for 20 min on ice. Cleared samples were precipitated with 10% TCA and subjected to Western blot analysis.

Cesium chloride and sucrose gradient purification of particles

Subviral particles of cellular supernatants were pelleted through a 1-ml cushion of 20% sucrose in TNE (10 mM Tris–CL [pH 7.5], 150 mM NaCl, 10 mM EDTA) using a SW 40 rotor (Beckman) at 37000 rpm for 4 h at 4 °C. The resuspended pellets were separated by isopycnic gradient centrifugation through 10–50% (wt/vol) cesium chloride in TNE. After centrifugation at 35000 rpm and 10 °C (SW 40 rotor), fractions were collected from the top and screened for chimeric particles by ELISA, immunoblotting, and fluorescence analysis. For velocity sedimentation, pelleted particles were layered on top of a 12-ml linear sucrose gradient (10 to 50% [wt/wt] sucrose in TNE buffer) with a 68% sucrose cushion, centrifuged at 35000 rpm and 10 °C for 16 h (SW 40 rotor), and processed as above.

Detection of extracellular virions

For replication of HBV in the HuH-7 liver cell line, plasmid pHBV was used that carries a 1.1 mer of the HBV DNA genome (Radziwill et al., 1990). This plasmid was co-transfected with pEGFP.S by the calcium phosphate precipitation technique. Four days after transfection, extra-cellular virions were separated from subviral empty enve-lopes and non-enveloped core particles by isopycnic CsCl gradient centrifugation. To this aim, 3.8 g of CsCl was dissolved in 10 ml cleared supernatant and 28 ml of this solution was spun for 20 h at 45 000 rpm at 10 °C in a Beckman 50vTi rotor. Fractions were collected from the bottom, supplemented with the protease inhibitor cocktail, and were screened for HBsAg and GFP by immunoassays. Following dialysis of fractions against 10 mM Tris–CL [pH 7.5], 150 mM NaCl at 4 °C, virions were isolated by an envelope-specific immunoprecipitation, as described previ-ously (Löffler-Mary et al., 2000). For detection of GFP.S within the virion envelope, particles were immunoprecipi-tated with the α-GFP MAb JL-8 that had been coated to a 10% (wt/vol) suspension of protein G-Sepharose (10-μl antibody was bound to 100 μl Sepharose solution in an overnight reaction at 4 °C). Immunoprecipitation was performed in the presence of 0.5% NP-40 and precipitates were then washed two times with TEN buffer (50 mM Tris–HCl [pH 7.5], 1 mM EDTA, 75 mM NH_4Cl). Detection of the encapsidated viral progeny DNA by radioactive labeling of the partially double-stranded genome with 10 μCi [$α^{32}P$]dATP (Amersham Biosciences) by the endogenous polymerase, isolation, and separation of the DNA by agarose gel electrophoresis have been described (Löffler-Mary et al., 2000). The radioactive signal was detected by PhosphorImager scanning.

For detection of HBV DNA on dot-blots, an *Eco*RI-linearized unit-length HBV genome was labeled with digoxygenin-dUTP by random priming as instructed by the manufacturer (Roche). After extraction of the DNA genomes from the immunoprecipitated samples as described, they were denatured by boiling in 0.4 M NaOH–10 mM EDTA and filtered with a dot-blot manifold (Schleicher and Schüll) onto nylon membranes. The membrane was baked at 120 °C for 30 min and hybridized with the labeled probe according to the Roche DIG DNA labeling and detection kit.

Binding assay

For binding analysis, human hepatoma HepG2 cells were cultivated in glass bottom dishes in Dulbecco's modified Eagle's medium with 10% fetal calf serum (FCS). HBV and subviral particles secreted from HuH-7 (co-)transfected cells were precipitated from 10-ml culture supernatant in the presence of 6% polyethylene glycol 8000 (PEG; Sigma). The pellet was resuspended in 200-μl phosphate-buffered saline (PBS) containing 25% FCS. HepG2 cells were

incubated with 50 μl of this concentrate, diluted in 1 ml culture medium with 4% PEG, for 20 h at 37 °C. Cells were washed three times with PBS and analyzed for GFP fluorescence by microscopy.

References

Berting, A., Hahnen, J., Kroger, M., Gerlich, W.H., 1995. Computer-aided studies on the spatial structure of the small hepatitis B surface protein. Intervirology 1–2, 8–15.

Bosch, B.J., De Haan, C.A., Rottier, P.J., 2004. Coronavirus spike glycoprotein, extended at the carboxy terminus with green fluorescent protein, is assembly competent. J. Virol. 78, 7369–7378.

Breiner, K.M., Urban, S., Schaller, H., 1998. Carboxypeptidase D (gp180), a golgi-resident protein, functions in the attachment and entry of avian hepatitis B viruses. J. Virol. 72, 8098–8104.

Bruss, V., Ganem, D., 1991. The role of envelope proteins in hepatitis B virus assembly. Proc. Natl. Acad. Sci. U.S.A. 88, 1059–1063.

Bruss, V., Lu, X., Thomssen, R., Gerlich, W.H., 1994. Post-translational alterations in transmembrane topology of the hepatitis B virus large envelope protein. EMBO J. 13, 2273–2279.

Bruss, V., Gerhardt, E., Vieluf, K., Wunderlich, G., 1996. Functions of the large hepatitis B virus surface protein in viral particle morphogenesis. Intervirology 39, 23–31.

Chisari, F.V., Filippi, P., McLachlan, A., Milich, D.R., Riggs, M., Lee, S., Palmiter, R.D., Pinkert, C.A., Brinster, R.L., 1986. Expression of hepatitis B virus large envelope polypeptide inhibits hepatitis B surface antigen secretion in transgenic mice. J. Virol. 60, 880–887.

Cooper, A., Paran, N., Shaul, Y., 2003. The earliest steps in hepatitis B virus infection. Biochim. Biophys. Acta 1614, 89–96.

Dalton, K.P., Rose, J.K., 2001. Vesicular stomatitis virus glycoprotein containing the entire green fluorescent protein on its cytoplasmic domain is incorporated efficiently into virus particles. Virology 279, 414–421.

Delpeyroux, F., Chenciner, N., Lim, A., Malpiece, Y., Blondel, B., Crainic, R., van der Werf, S., Streeck, R.E., 1986. A poliovirus neutralization epitope expressed on hybrid hepatitis B surface antigen particles. Science 233, 472–475.

Desai, P., Person, S., 1998. Incorporation of the green fluorescent protein into the herpes simplex virus type 1 capsid. J. Virol. 72, 7563–7568.

Gripon, P., Diot, C., Guguen-Guillouzo, C., 1993. Reproducible high level infection of cultured adult human hepatocytes by hepatitis B virus: effect of polyethylene glycol on adsorption and penetration. Virology 192, 534–540.

Gripon, P., Rumin, S., Urban, S., Le Seyec, J., Glaise, D., Cannie, I., Guyomard, C., Lucas, J., Trepo, C., Guguen-Guillouzo, C., 2002. Infection of a human hepatoma cell line by hepatitis B virus. Proc. Natl. Acad. Sci. U.S.A. 99, 15655–15660.

Hagelstein, J., Fathinejad, F., Stremmel, W., Galle, P.R., 1997. pH-independent uptake of hepatitis B virus in primary human hepatocytes. Virology 229, 292–294.

Hartmann-Stühler, C., Prange, R., 2001. Hepatitis B virus large envelope protein interacts with g2-adaptin, a clathrin adaptor-related protein. J. Virol. 75, 5343–5351.

Heermann, K.H., Gerlich, W.H., 1991. Surface proteins of hepatitis B viruses. In: McLachlan, A. (Ed.), Molecular Biology of the Hepatitis B Virus. CRC Press, Boca Raton, FL, pp. 109–143.

Huovila, A.P., Eder, A.M., Fuller, S.D., 1992. Hepatitis B surface antigen assembles in a post-ER, pre-Golgi compartment. J. Cell Biol. 118, 1305–1320.

Köck, J., Nassal, M., MacNelly, S., Baumert, T.F., Blum, H.E., von Weizsacker, F., 2001. Efficient infection of primary tupaia hepatocytes with purified human and woolly monkey hepatitis B virus. J. Virol. 75, 5084–5089.

Lambert, C., Prange, R., 2001. Dual topology of the hepatitis B virus large envelope protein: determinants influencing post-translational pre-S translocation. J. Biol. Chem. 276, 22265–22272.

Le Seyec, J., Chouteau, P., Cannie, I., Guguen-Guillouzo, C., Gripon, P., 1999. Infection process of the hepatitis B virus depends on the presence of a defined sequence in the pre-S1 domain. J. Virol. 73, 2052–2057.

Löffler-Mary, H., Dumortier, J., Klentsch-Zimmer, C., Prange, R., 2000. Hepatitis B virus assembly is sensitive to changes in the cytosolic S loop of the envelope proteins. Virology 270, 358–367.

Lu, X., Block, T.M., Gerlich, W.H., 1996. Protease-induced infectivity of hepatitis B virus for human hepatoblastoma cell line. J. Virol. 70, 2277–2285.

Michel, M.-L., Mancini, M., Sobczak, E., Favier, V., Guetard, D., Bahraoui, E.M., Tiollais, P., 1988. Induction of anti-human immunodeficiency virus (HIV) neutralizing antibodies in rabbits immunized with recombinant HIV-hepatitis B surface antigen particles. Proc. Natl. Acad. Sci. U.S.A. 85, 7957–7961.

Nassal, M., 1996. Hepatitis B virus morphogenesis. CMTI, 297–337.

Neurath, A.R., Kent, S.B.H., Strick, N., Parker, K., 1986. Identification and chemical synthesis of a host cell receptor binding site on hepatitis B virus. Cell 46, 429–436.

Okiyoneda, T., Harada, K., Takeya, M., Yamahira, K., Wada, I., Shuto, T., Suico, M.A., Hashimoto, Y., Kai, H., 2004. ΔF508 CFTR pool in the endoplasmic reticulum is increased by calnexin overexpression. MBC 15, 563–574.

Ostapchuk, P., Hearing, P., Ganem, D., 1994. A dramatic shift in the transmembrane topology of a viral envelope glycoprotein accompanies hepatitis B viral morphogenesis. EMBO J. 13, 1048–1057.

Prange, R., Streeck, R.E., 1995. Novel transmembrane topology of the hepatitis B virus envelope proteins. EMBO J. 14, 247–256.

Prange, R., Nagel, R., Streeck, R.E., 1992. Deletions in the hepatitis B virus small envelope protein: effect on assembly and secretion of surface antigen particles. J. Virol. 66, 5832–5841.

Prange, R., Werr, M., Birkner, M., Hilfrich, R., Streeck, R.E., 1995. Properties of modified hepatitis B virus surface antigen particles carrying preS epitopes. J. Gen. Virol. 76, 2131–2140.

Radziwill, G., Tucker, W., Schaller, H., 1990. Mutational analysis of the hepatitis B virus P gene product: domain structure and RNase H activity. J. Virol. 64, 613–620.

Simon, K., Lingappa, V.R., Ganem, D., 1988. Secreted hepatitis B surface antigen polypeptides are derived from a transmembrane precursor. J. Cell Biol. 107, 2163–2168.

Stauber, R.H., Rulong, S., Palm, G., Tatasova, N.I., 1999. Direct visualization of HIV-1 entry: mechanisms and role of cell surface receptors. Biochem. Biophys. Res. Commun. 258, 695–702.

Stirk, H.J., Thornton, J.M., Howard, C.R., 1992. A topological model for hepatitis B surface antigen. Intervirology 33, 148–158.

Ward, B.M., Moss, B., 2001. Visualization of intracellular movement of vaccinia virus virions containing a green fluorescent protein-B5R membrane protein chimera. J. Virol. 75, 4802–4813.

Wunderlich, G., Bruss, V., 1996. Characterization of early hepatitis B virus surface protein oligomers. Arch. Virol. 141, 1191–1205.